Transcritical flow of a stratified fluid: The forced extended Korteweg–de Vries model

R. H. J. Grimshaw
Department of Mathematical Sciences, Loughborough University, Loughborough, Leicestershire, LE11 3TU, United Kingdom

K. H. Chan and K. W. Chow
Department of Mechanical Engineering, University of Hong Kong, Pokfulam Road, Hong Kong

(Received 19 June 2001; accepted 2 November 2001)

Transcritical, or resonant, flow of a stratified fluid over an obstacle is studied using a forced extended Korteweg–de Vries model. This model is particularly relevant for a two-layer fluid when the layer depths are near critical, but can also be useful in other similar circumstances. Both quadratic and cubic nonlinearities are present and they are balanced by third-order dispersion. We consider both possible signs for the cubic nonlinear term but emphasize the less-studied case when the cubic nonlinear term and the dispersion term have the same-signed coefficients. In this case, our numerical computations show that two kinds of solitary waves are found in certain parameter regimes. One kind is similar to those of the well-known forced Korteweg–de Vries model and occurs when the cubic nonlinear term is rather small, while the other kind is irregularly generated waves of variable amplitude, which may continually interact. To explain this phenomenon, we develop a hydraulic theory in which the dispersion term in the model is omitted. This theory can predict the occurrence of upstream and downstream undular bores, and these predictions are found to agree quite well with the numerical computations. © *2002 American Institute of Physics.* [DOI: 10.1063/1.1429962]

I. INTRODUCTION

The evolution of weakly nonlinear long waves, in both homogeneous and density-stratified fluid environments, is of great interest in many branches of fluid mechanics, notably in oceanographic applications. When the leading balance is between quadratic nonlinearity and dispersion, the dynamics is typically governed by the well-known Korteweg–de Vries (KdV) equation. For larger waves, or for certain special configurations in stratified fluids, it has been found useful to include cubic nonlinearity, leading to the extended KdV (eKdV) equation. Such model systems have been derived in the literature for stratified fluids, and the localized solitary waves have been identified (see, for instance, the review article by Grimshaw,[1] as well as the recent more specialized works by Holloway *et al.*,[2] Michalet and Barthelemy,[3] and Grimshaw *et al.*[4])

In many geophysical and marine applications it is necessary to include a forcing term; typical examples are when the waves are generated by moving ships, or by flow over bottom topography. Previous studies[2–8] have identified some interesting features of the forced eKdV equation. These include undular bores propagating upstream in the subcritical regime, and monotonic bores in the transcritical regime; such bores may remain stationary. These features differ sharply from the solution of the forced KdV equation, where in the transcritical regime solitary waves are generated continually and propagate upstream. Locally steady flow is observed for sufficiently large Froude numbers in the supercritical range of such eKdV systems, while stationary lee waves are formed for sufficiently low Froude numbers in the subcritical regime. For the forced KdV equation Grimshaw and Smyth[8] (GS) showed that the upstream and downstream wave trains could be well described by the modulation theory for the KdV equation, which, in turn, is a development from the hydraulic approximation in which the dispersive term is neglected. However, it seems that the modulation theory for the eKdV equation is not fully available, except for sufficiently small-amplitude waves.[6]

Further, numerical simulations of the full equations for stratified flow over topography have been performed for a two-layer stratification and for a linearly stratified Boussinesq fluid.[7–12] Flows past an obstacle in a horizontal channel will reach criticality if the linear long wave speed of one mode is equal to the upstream flow speed. The energy of the waves excited by the obstacle cannot propagate away from it, and hence a strongly nonlinear response occurs. Indeed it is this feature that leads to the necessity for such nonlinear theoretical models as those provided by the forced KdV and eKdV equations. These full numerical simulations broadly support the behavior types seen in the model equations. Further, we note that a forced eKdV equation has been discussed in the context of the generation of capillary-gravity waves in a two-layer fluid;[11] also, a set of coupled forced KdV equations have been discussed for surface waves, with a view to retaining a (weak) interaction with the nonresonant wave mode.[9]

It is known that the solutions of the eKdV equation will depend on the relative signs of the coefficient of the cubic nonlinear and dispersive terms. Most studies of the forced

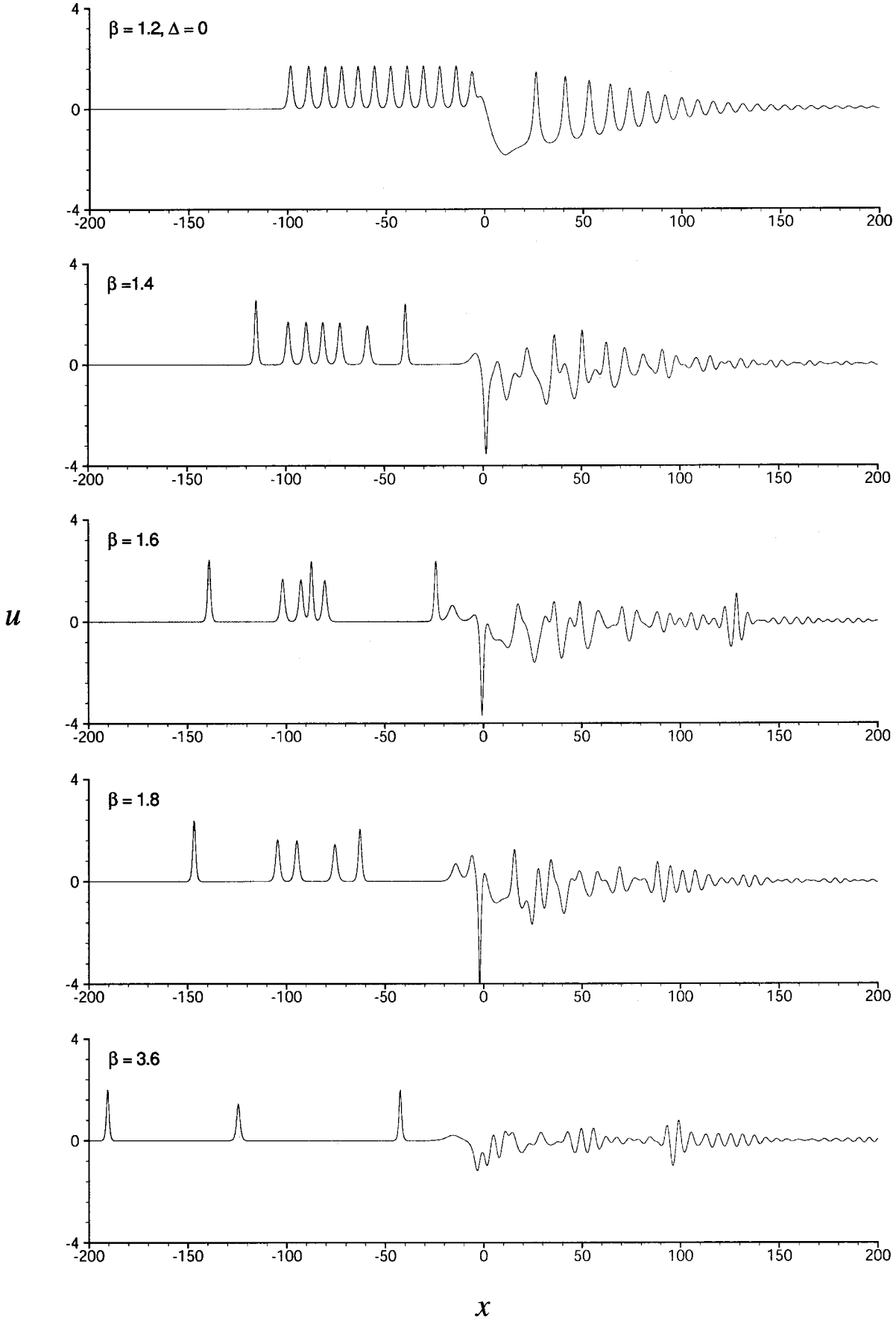

FIG. 1. The interfacial displacement at $t=60$ with $\Delta=0$, $f_m=1.0$, and $\xi=0.3$ for $\beta>0$.

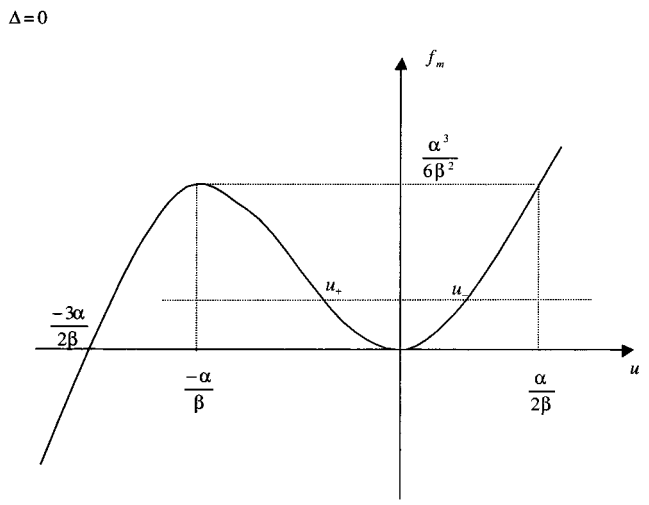

FIG. 2. Here f_m vs u for $\Delta=0$.

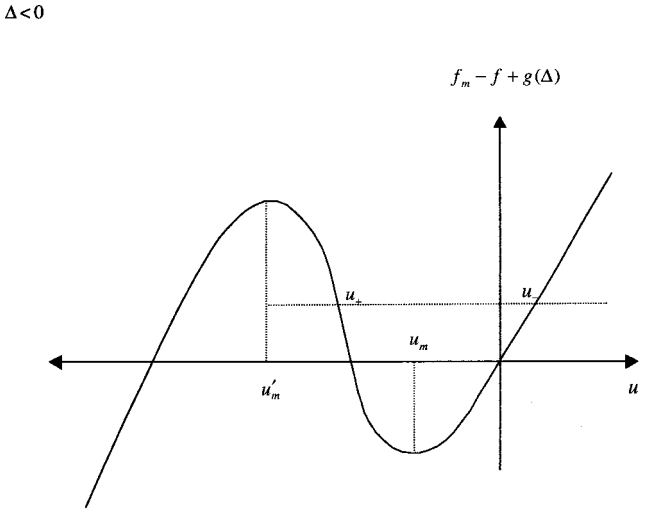

FIG. 3. Here $f_m - f + g(\Delta)$ vs u for $\Delta \neq 0$, for $\Delta < 0$. The case $\Delta > 0$ is similar.

eKdV equation mentioned above, with one exception,[11] deal with the case where these terms are of opposite sign. In this case the eKdV equation supports a single family of solitary waves, whose polarity is determined by the relative signs of the coefficient of the quadratic nonlinear and dispersive terms, which for small amplitudes resemble those of the KdV equation, but for large amplitudes become ''thick'' solitary waves with a limiting amplitude.[1] On the other hand, when the cubic nonlinear and dispersive terms have the same-signed coefficients, the eKdV equation supports two families of solitary waves; one resembles the KdV solitary waves at small amplitudes, but the other, with opposite polarity, can exist only for large amplitudes. Since the coefficient of the cubic nonlinear term in the eKdV equation can have either sign for various layered and stratified fluids,[10,11] our objective in the present work is to study waves generated by the forced eKdV for both signs of the cubic nonlinear term, with a particular emphasis on the less-studied case when the cubic nonlinear and dispersive terms have the same sign. As the procedure for deriving such a forced eKdV equation is standard,[1,5,6] and well known, we shall proceed directly with a study of a nondimensional forced eKdV equation. Formats and signs for this forced eKdV will conform as far as possible with the forms used in earlier studies.

The strategy will be a combined analytical and computational study. First, based on the usefulness of the hydraulic approximation used by GS[8] in their study of the forced KdV equation, an analogous hydraulic approximation for the forced eKdV equation will be developed here and used to study the transcritical regime. Second, the forced eKdV equation will be solved numerically, and the results compared with the hydraulic approximation. The most interesting result is that two kinds of solitary waves can be emitted and travel upstream in certain parameter regimes. The first type is generated at regular intervals when the cubic nonlinear term is relatively unimportant, while the second type is produced irregularly and occurs when the cubic nonlinear term plays a crucial role.

II. FORCED EXTENDED KORTEWEG-de VRIES EQUATION

We begin the analytical formulation by considering the forced eKdV equation for an appropriate field variable $u(x,t)$,

$$\frac{\partial u}{\partial t} + \Delta \frac{\partial u}{\partial x} - \alpha u \frac{\partial u}{\partial x} - \beta u^2 \frac{\partial u}{\partial x} - \frac{\partial^3 u}{\partial x^3} = \frac{\partial f}{\partial x}. \tag{1}$$

For instance, in a two-layer fluid, u is the interfacial displacement.[1] Here Δ measures the deviation from the long wave phase speed, and is the parameter that controls the flow regime; $f(x)$ is the representation of the localized topographic forcing; α and β are the coefficients of the quadratic and cubic nonlinear terms, respectively, and can be determined explicitly in terms of the basic state of the stratified fluid.[1,5,7,8,10] For an initial condition, we set $u(x,0)=0$, which corresponds to turning on the basic flow at the initial time. The forcing function used in our numerical simulations is

$$f = f_m \exp(-\xi^2 x^2), \tag{2}$$

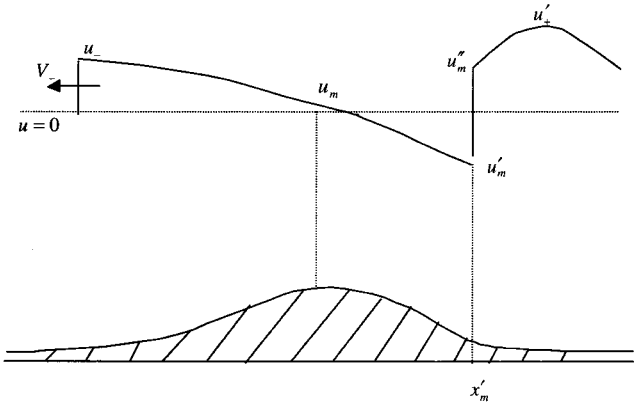

FIG. 4. Configuration for a stationary downstream shock.

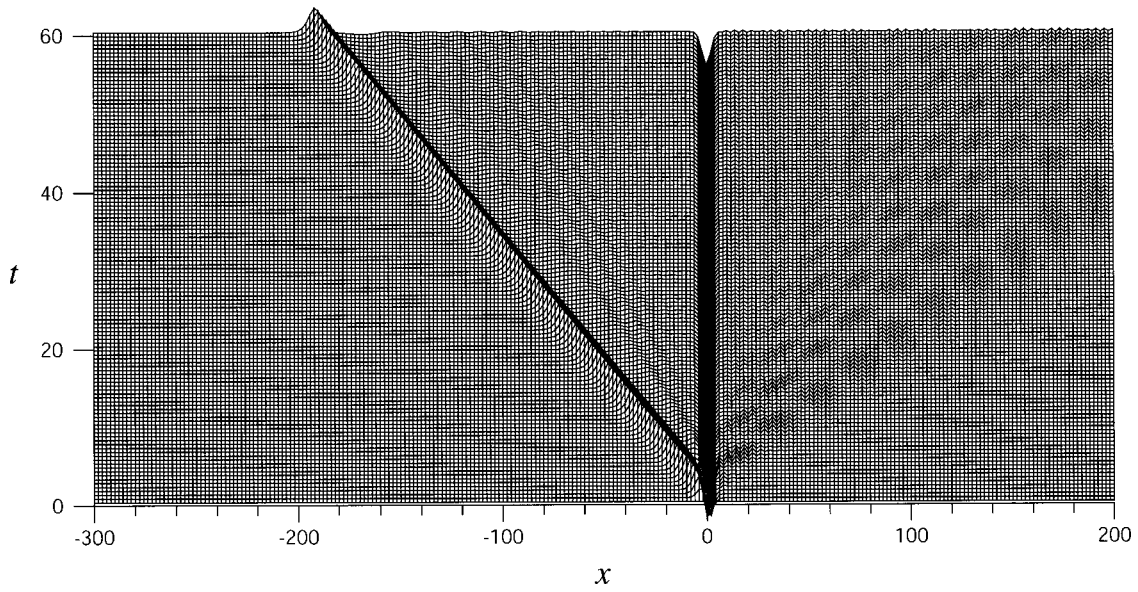

FIG. 5. The numerical solution with $\Delta=-3.0$, $\beta=1.4$, $f_m=1.0$, and $\xi=0.3$.

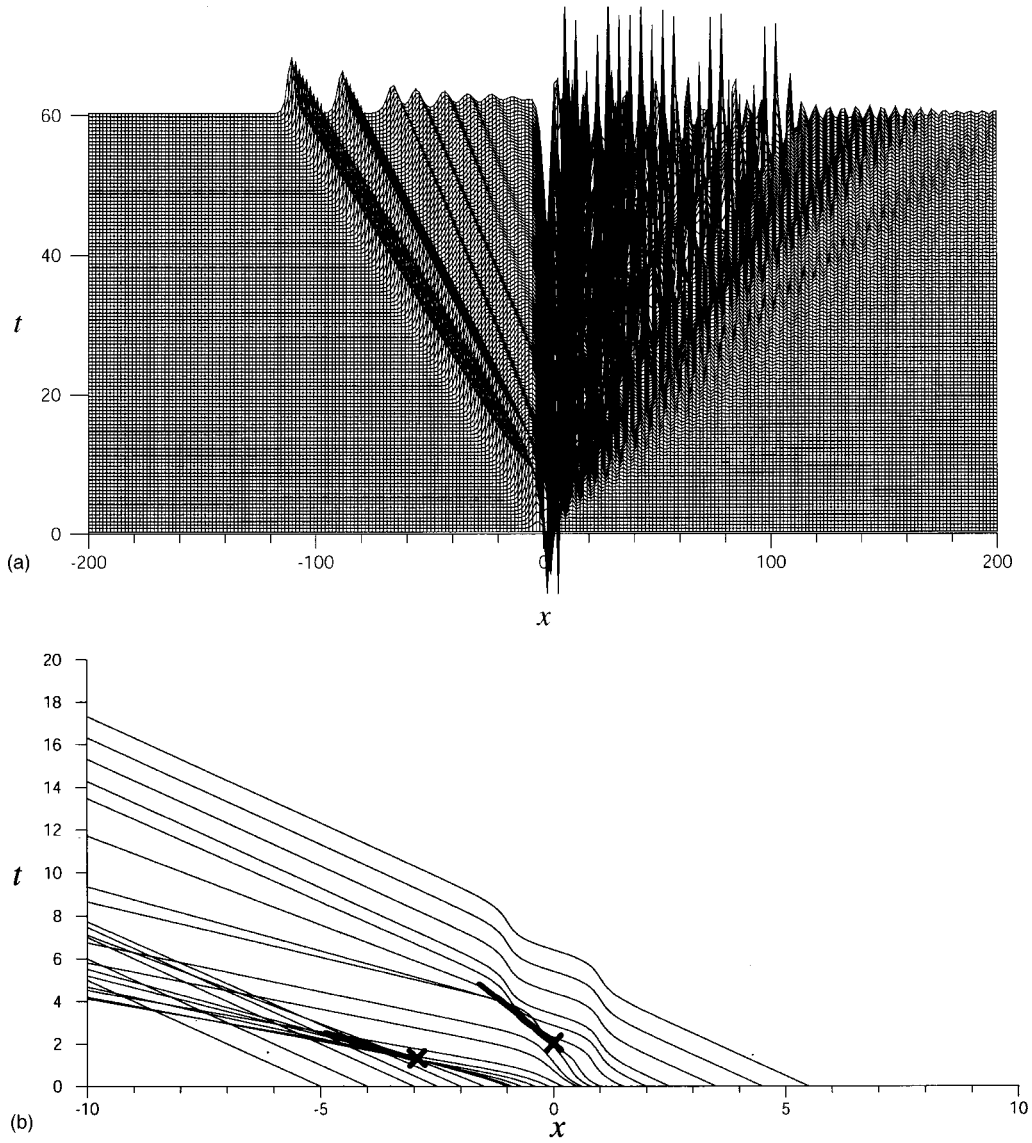

FIG. 6. (a) The numerical solution with $\Delta=-1.0$, $\beta=1.4$, $f_m=1.0$, and $\xi=0.3$. (b) The characteristics configuration for the hydraulic approximation with $\Delta=-1.0$, $\beta=1.4$, $f_m=1.0$, and $\xi=0.3$. (c) The interfacial displacement of the flow at $t=60$ with $\Delta=-1.0$, $f_m=1.0$, and $\xi=0.3$ for $\beta>0$.

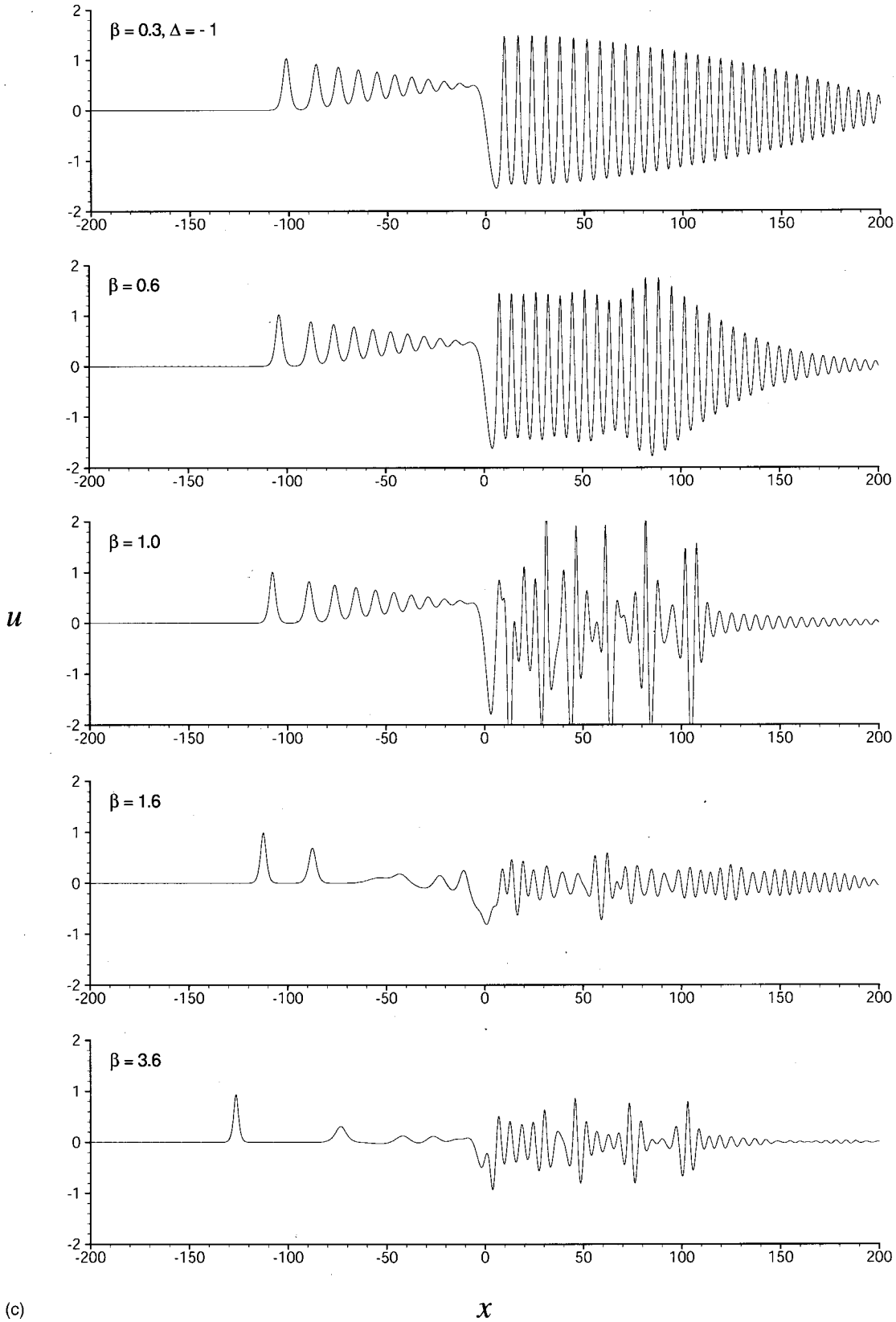

FIG. 6. (*Continued.*)

where ξ is a shape parameter. In general, we assume that f has a single maximum and decays rapidly in the farfield. Only positive forcing is considered in this study, [i.e., $f_m > 0$ in Eq. (2)] and α is kept constant (equal to 2 without loss of generality) for all the numerical computations. However, we vary the coefficient β and allow it to be both positive and negative. A typical sequence of numerical computations for $\Delta = 0$, $f_m = 1$ is shown in Fig. 1 for $\beta > 0$.

III. HYDRAULIC APPROXIMATION

To explain the features shown in Fig. 1 and all our other numerical computations, we follow the approach of GS[8] and consider here the hydraulic approximation. Formally this is valid for broad forcings [$\xi \to 0$ in Eq. (2)], and can be expected to lead to a combination of locally steady-state solutions together with shocks. As in GS, we expect the shocks to be indicative of the presence of wave trains in the full equations (1), although, as far as we aware, there is currently no counterpart for the eKdV equation to the modulation theory for the KdV equation used by GS. On omission of the dispersive term, Eq. (1) becomes

$$\frac{\partial u}{\partial t} + \Delta \frac{\partial u}{\partial x} - \alpha u \frac{\partial u}{\partial x} - \beta u^2 \frac{\partial u}{\partial x} = \frac{\partial f}{\partial x}. \tag{3}$$

Equation (3) can be solved by the method of characteristics. These are given by

$$\frac{dx}{dt} = \Delta - \alpha u - \beta u^2, \quad \frac{du}{dt} = \frac{\partial f}{\partial x}, \tag{4}$$

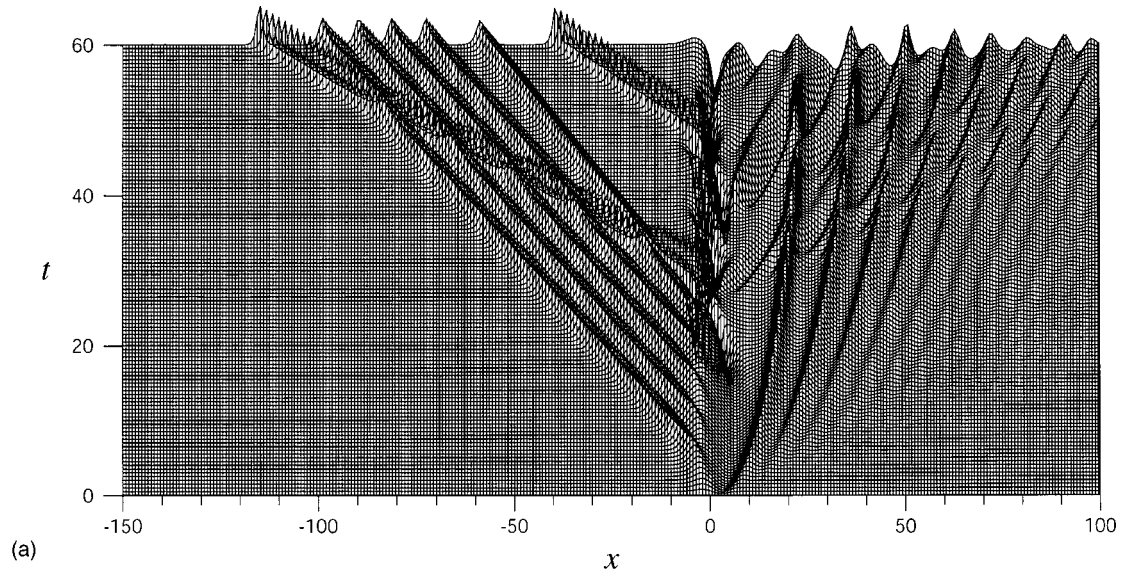

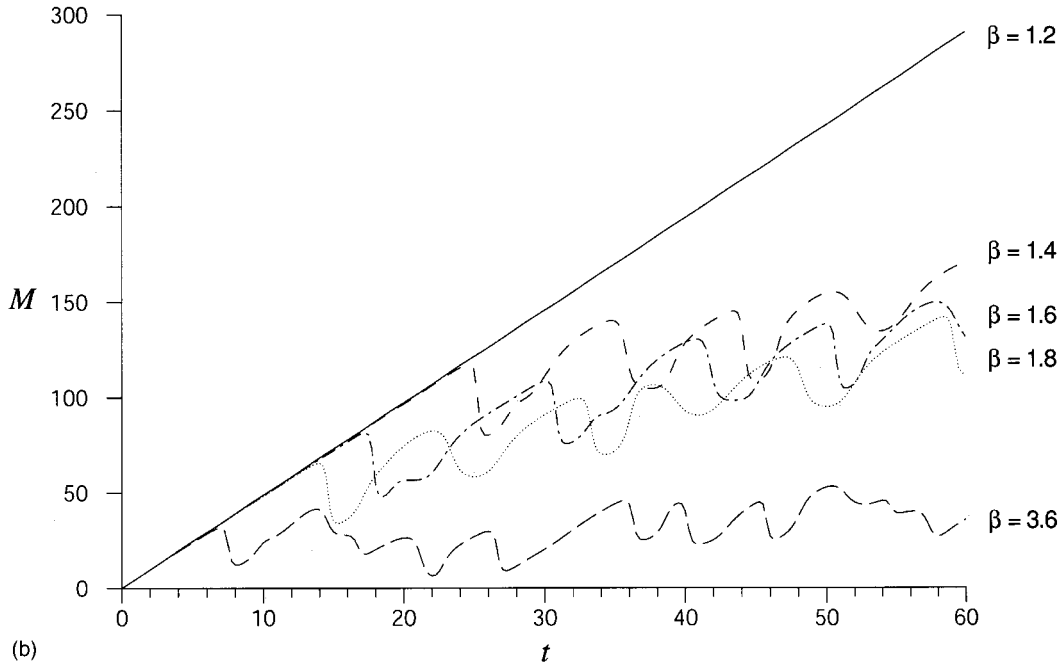

FIG. 7. (a) The numerical solution with $\Delta = 0$, $\beta = 1.4$, $f_m = 1.0$, and $\xi = 0.3$. (b) The mass fluctuations with $\Delta = 0$, $f_m = 1.0$, and $\xi = 0.3$ (only M_{front} is shown). (c) The characteristics configuration for the hydraulic approximation with $\Delta = 0$, $\beta = 1.4$, $f_m = 1.0$, and $\xi = 0.3$.

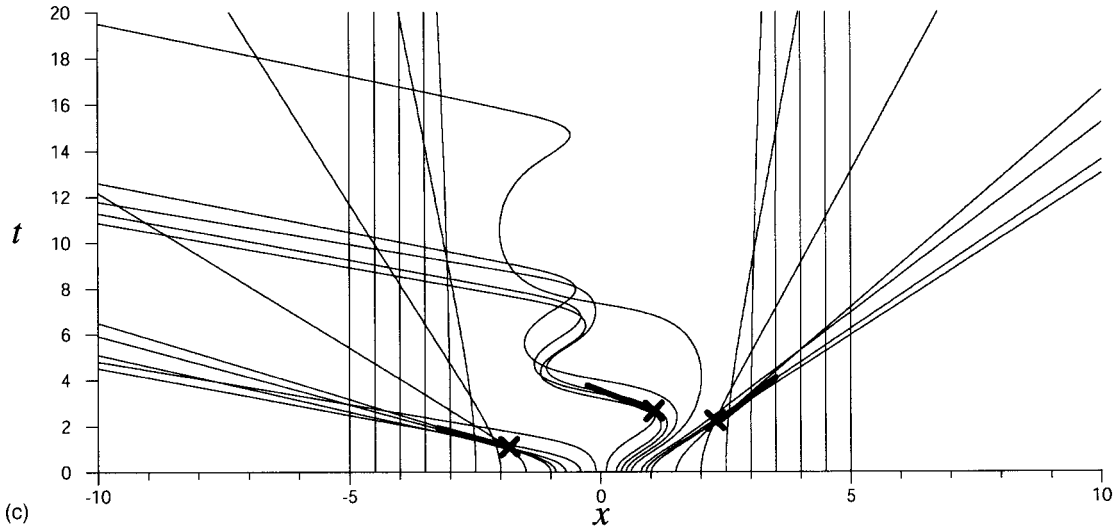

FIG. 7. (*Continued.*)

.

where on a given characteristic at $t=0$, $x=x_0$, $u=0$. Here x_0 is a parameter defining each characteristic. Equations (4) are readily solved numerically, although we note that analytically the solution can be written in the form

$$\Delta u - \tfrac{1}{2}\alpha u^2 - \tfrac{1}{3}\beta u^3 = f(x) - f(x_0), \tag{5}$$

which gives u in terms of x and x_0. Substitution into the first of Eqs. (4) then gives $x=x(x_0,t)$, and the subsequent elimination of x_0 then yields the solution of Eq. (3). However, if the characteristics intersect, then a shock much be inserted. The shock speed V can be determined by integrating Eq. (3) across the shock, and is

$$V=\Delta-\tfrac{1}{2}\alpha(u_a+u_b)-\tfrac{1}{3}\beta(u_a^2+u_a u_b+u_b^2), \tag{6}$$

where $u_{a,b}$ are the values of u on each side of the shock. However, in our numerical solutions of Eqs. (4) we allow the characteristics to intersect, and the shocks are inserted only schematically, i.e., we determine numerically the points (X) where characteristics first intersect, and sketch a curve (solid line) whose slope at the initial intersection point is given by Eq. (6).

Next, to determine the criteria for a steady hydraulic solution, we ignore the unsteady term in Eq. (3) which then becomes

$$\Delta\frac{\partial u}{\partial x}-\alpha u\frac{\partial u}{\partial x}-\beta u^2\frac{\partial u}{\partial x}=\frac{\partial f}{\partial x}. \tag{7}$$

We shall assume that $\alpha>0$ without loss of generality, and also in the subsequent discussion, we shall assume that $\beta>0$. The case $\beta<0$ can be recovered by the transformation $u\to -u$, $\Delta\to-\Delta$. At the local maximum of the forcing, located at $x=0$, $f(0)=f_m$, $f_x=0$ and we let $u=u_m$. Then Eq. (7) shows that either $u_x=0$, or that

$$\Delta=\alpha u_m+\beta u_m^2, \quad \text{i.e.,} \quad \beta u_m=-\frac{\alpha}{2}\pm\left\{\frac{\alpha^2}{4}+\Delta\beta\right\}^{1/2}. \tag{8}$$

Since we are interested only in asymmetric steady hydraulic solutions, we assume here that $u_x\neq 0$ at $x=0$, and so Eq. (8) holds; later we will show that only the upper sign in Eq. (8) is relevant. In the farfield, where $f\to 0$ we let $u\to u_\pm$, where u_- and u_+ represent the upstream ($x\to-\infty$) and downstream ($x\to+\infty$) values, respectively, and we will require that $u_+\neq u_-$. Later we will show that $u_->u_+$. Integrating Eq. (7) with respect to x gives

$$\Delta u-\frac{\alpha u^2}{2}-\frac{\beta u^3}{2}-f=C, \tag{9}$$

where C can be determined by the farfield conditions, or by the condition at $x=0$, so that

$$C=\Delta u_\pm-\frac{\alpha}{2}u_\pm^2-\frac{\beta}{3}u_\pm^3=\Delta u_m-\frac{\alpha u_m^2}{2}-\frac{\beta u_m^3}{3}-f_m. \tag{10}$$

Further, since $u_-\neq u_+$, we obtain

$$\Delta=\frac{\alpha}{2}(u_++u_-)+\frac{\beta}{3}(u_+^2+u_+u_-+u_-^2). \tag{11}$$

First, for simplicity, let $\Delta=0$. In this case, Eq. (8) implies that $u_m=0$, or $u_m=-\alpha/\beta$. If $u_m=0$, then $C=-f_m$ and the solution of Eq. (9) becomes

$$f_m-f=\tfrac{1}{2}\alpha u^2+\tfrac{1}{3}\beta u^3,$$

which is plotted in Fig. 2. Clearly,

$$\frac{\alpha}{2}u_\pm^2+\frac{\beta}{3}u_\pm^3=f_m<\frac{\alpha^3}{6\beta^2} \tag{12}$$

must hold for this solution to exist and, furthermore,

$$\frac{\alpha}{2\beta}>u_->0>u_+>-\frac{\alpha}{\beta}.$$

In the other case, if $u_m=-\alpha/\beta$, it can be shown that there is no solution, most obviously by again using Fig. 2.

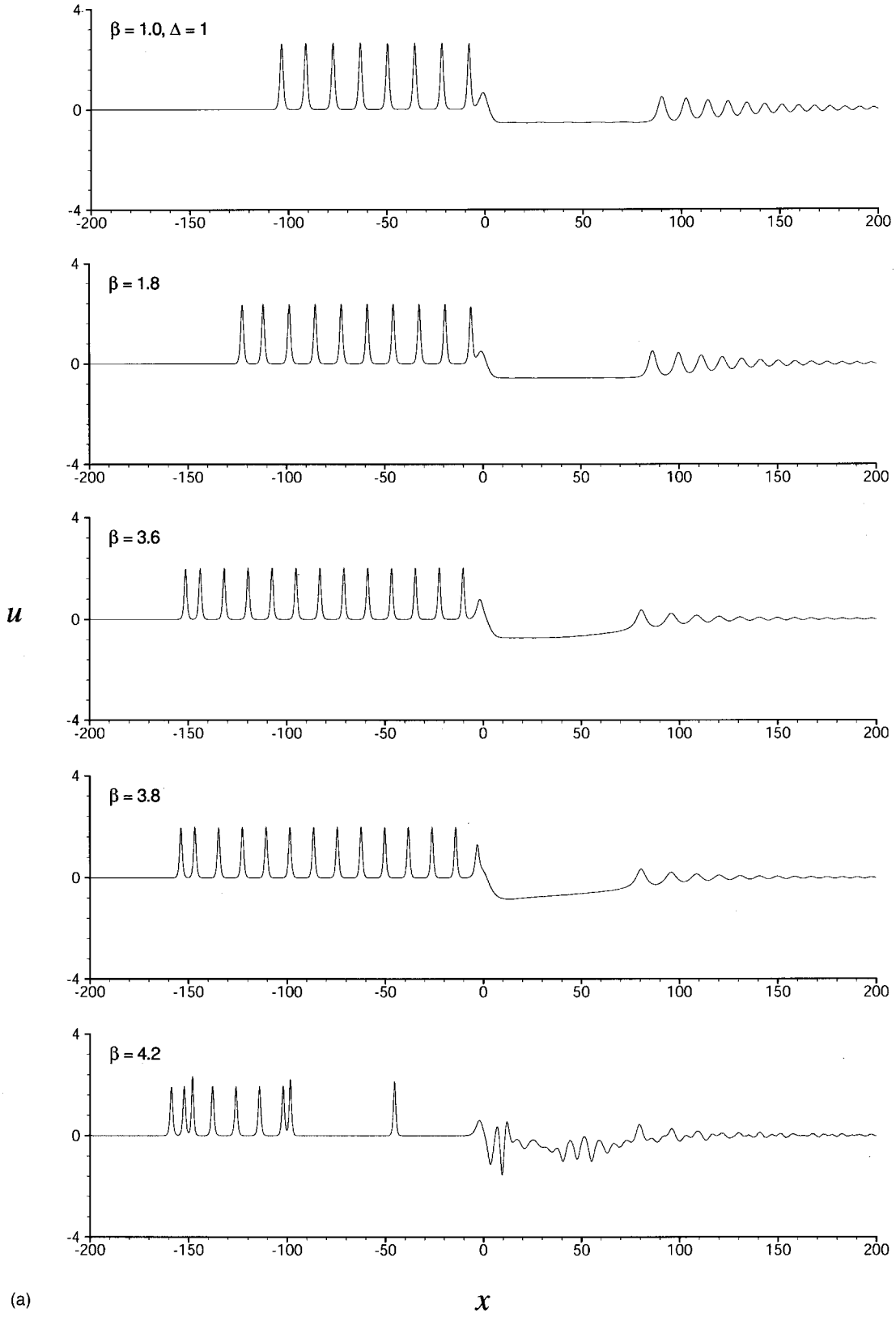

FIG. 8. (a) The interfacial displacement at $t=60$ with $\Delta=1.0$, $f_m=1.0$, and $\xi=0.3$ for $\beta>0$. (b) The numerical solution with $\Delta=1.0$, $\beta=4.2$, $f_m=1.0$, and $\xi=0.3$. (c) The interfacial displacement at $t=60$ with $\Delta=2.0$, $f_m=1.0$, and $\xi=0.3$ for $\beta>0$. (d) The numerical solution with $\Delta=3.0$, $\beta=1.4$, $f_m=1.0$, and $\xi=0.3$.

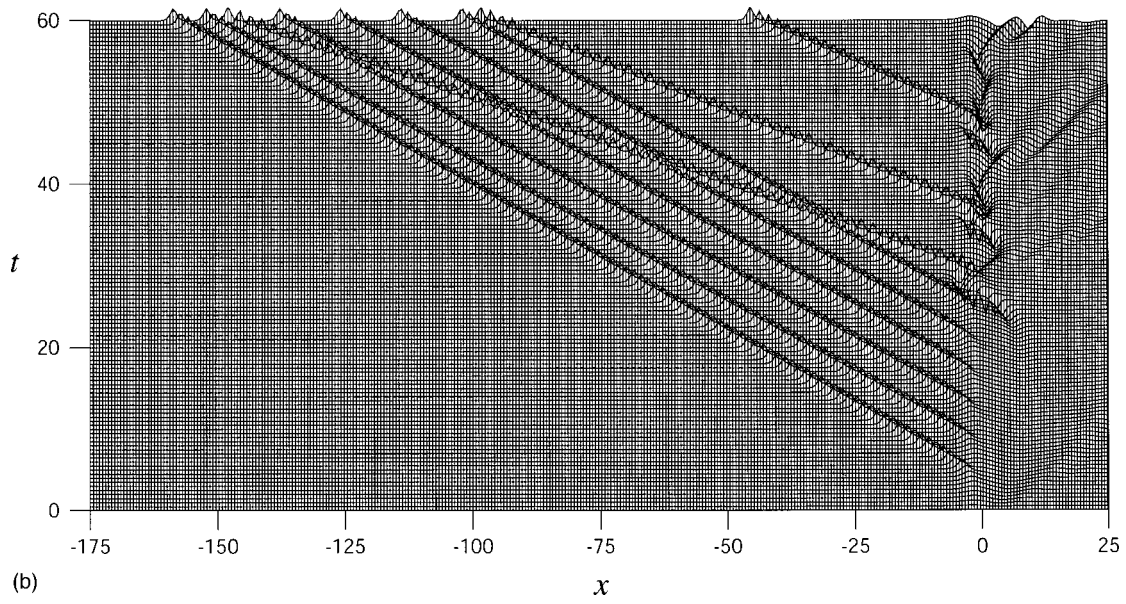

FIG. 8. (*Continued.*)

.

Then, in the general case, we consider $\Delta \neq 0$ for $\alpha > 0$, $\beta > 0$. First Eq. (8) shows that u_m will not exist unless

$$\Delta > -\frac{\alpha^2}{4\beta}. \tag{13}$$

Since $u_m = 0$ when $\Delta = 0$, we choose u_m by the upper sign in Eq. (8). Equations (9) and (10) then give

$$f_m - f + g(\Delta) = -\Delta u + \frac{\alpha u^2}{2} + \frac{\beta u^3}{3}, \tag{14}$$

where

$$g(\Delta) = -\Delta u_m + \frac{\alpha}{2} u_m^2 + \frac{\beta}{3} u_m^3, \quad \text{or}$$

$$g(\Delta) = \frac{\alpha\Delta}{2\beta} + \frac{\alpha^3}{12\beta^2} - \frac{2}{3\beta^2}\left\{\frac{\alpha^2}{4} + \Delta\beta\right\}^{3/2}.$$

We now plot $f_m - f^+ g(\Delta)$ as a function of u in Fig. 3, and see that there are two turning points:

$$u = u_m, \quad u_m = -\frac{\alpha}{2\beta} + \frac{1}{\beta}\left\{\frac{\alpha^2}{4} + \Delta\beta\right\}^{1/2}$$

(a local minimum), (15)

$$u = u_m', \quad u_m' = -\frac{\alpha}{2\beta} - \frac{1}{\beta}\left\{\frac{\alpha^2}{4} + \Delta\beta\right\}^{1/2},$$

(a local maximum). (16)

Thus, a solution with $u_- > u_m > u_+$ exists until f_m reaches a value, such that

$$f_m = -\Delta(u_m' - u_m) + \frac{\alpha}{2}(u_m'^2 - u_m^2) + \frac{\beta}{3}(u_m'^3 - u_m^3)$$

$$= -g(\Delta) - \Delta u_m' + \frac{\alpha}{2} u_m'^2 + \frac{\beta}{3} u_m'^3. \tag{17}$$

From Eqs. (15) and (16),

$$u_m' - u_m = -\frac{2}{\beta}\left\{\frac{\alpha^2}{4} + \Delta\beta\right\}^{1/2}, \quad u_m' + u_m = -\frac{\alpha}{\beta},$$

and we find that this hydraulic solution exists, provided that

$$f_m \leqslant \frac{4}{3\beta^2}\left\{\frac{\alpha^2}{4} + \Delta\beta\right\}^{3/2}. \tag{18}$$

Note here that

$$g(\Delta) = \frac{\alpha^3}{12\beta^2}\left[1 + \frac{6\Delta\beta}{\alpha^2} - \left(1 + \frac{4\Delta\beta}{\alpha^2}\right)^{3/2}\right] \leqslant 0, \tag{19}$$

holds for all Δ in the allowed range, $\Delta > -\alpha^2/4\beta$ and $g(\Delta) = 0$ at $\Delta = 0$.

The shock velocities upstream (V_-) and downstream (V_+) are found from Eq. (6) with $u_{a,b} = (0, u_-)$ and $(0, u_+)$, respectively, so that

$$V_\pm = \Delta - \frac{\alpha u_\pm}{2} - \frac{\beta u_\pm^2}{3} = \frac{-[f_m + g(\Delta)]}{u_\pm}.$$

Since we require that $V_+ > 0 > V_-$, it follows that $u_- > 0 > u_+$ and that (see Fig. 3)

$$f_m > -g(\Delta), \tag{20}$$

which defines the transcritical regime. The results Eq. (18) and Eq. (20) are the main conclusion from this study of the steady hydraulic solutions. Equation (18) is the condition for the existence of the downstream steady state u_+, while Eq. (20), together with Eq. (13), define the range of Δ for which

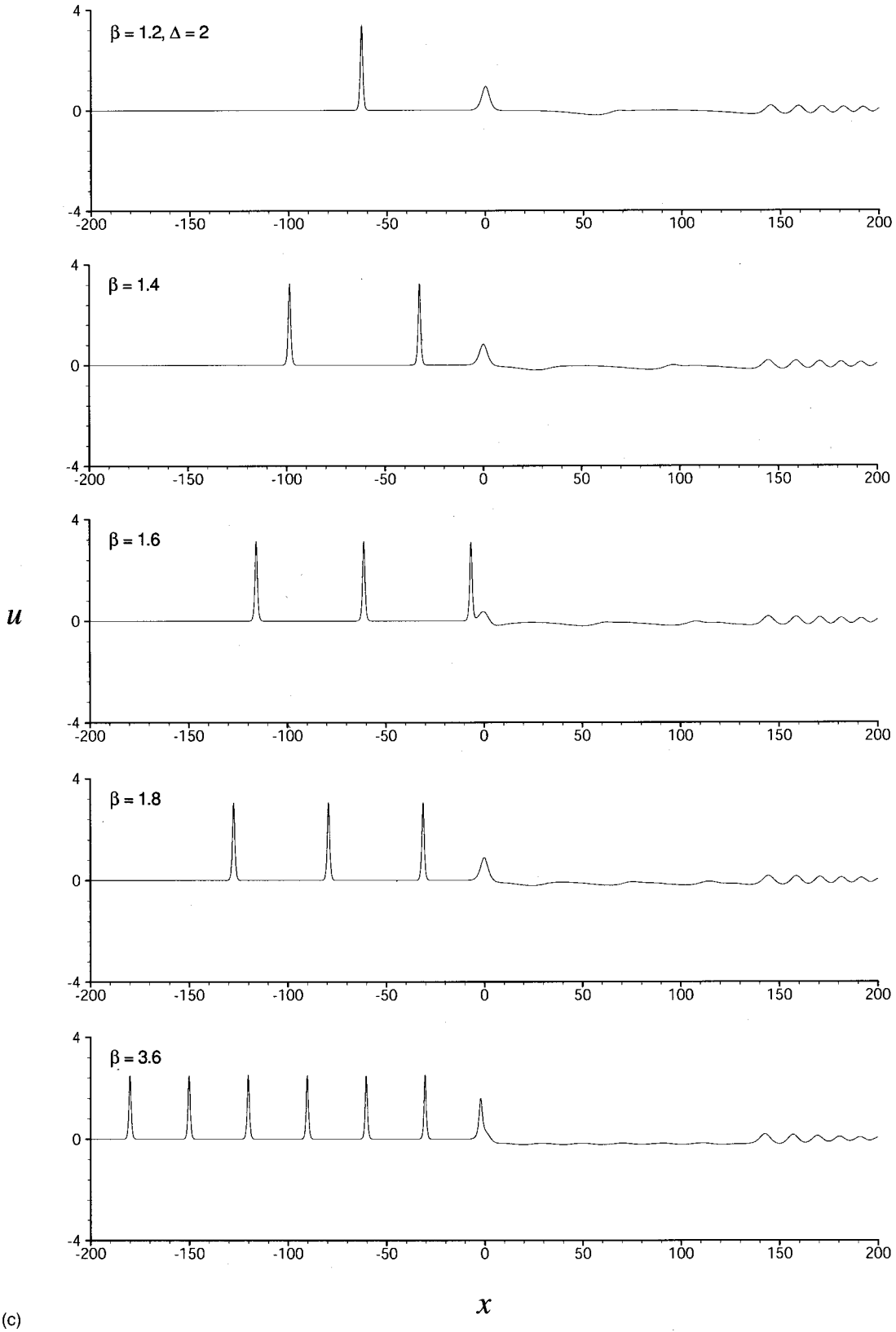

(c)

FIG. 8. (*Continued.*)

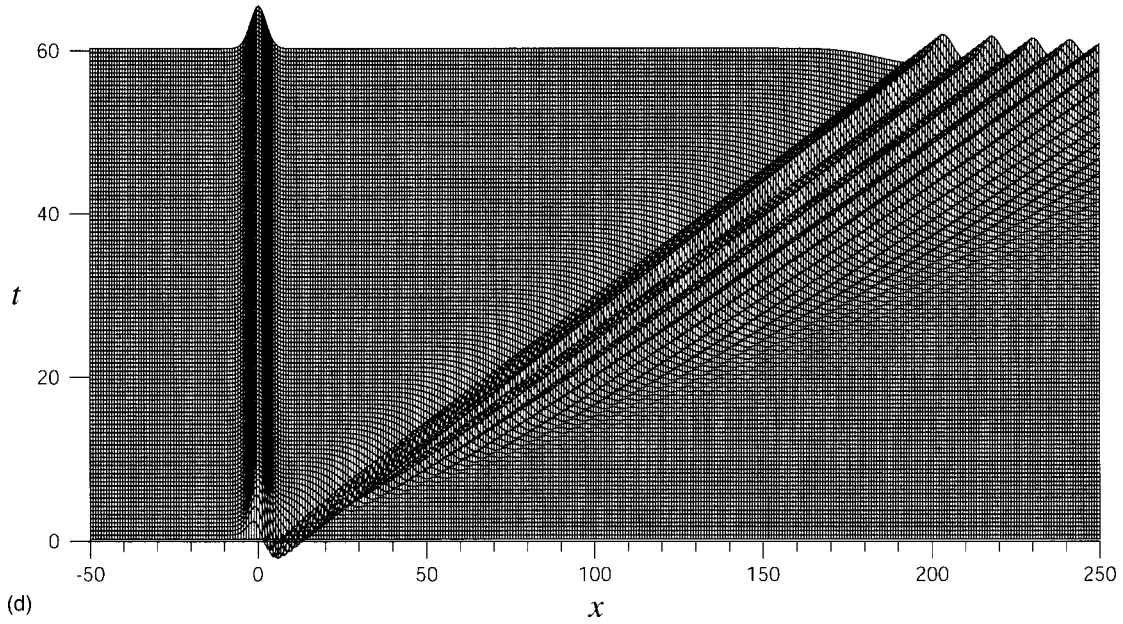

FIG. 8. (*Continued.*)

.

this asymmetric hydraulic solution can be obtained. We reiterate that when both Eq. (18) and Eq. (20) are satisfied we anticipate that in the full equation (1) the shocks $u_{\pm}$ are replaced by wave trains, as in GS.

The case

$$f_m > \frac{4}{3\beta^2}\left(\frac{\alpha^2}{4}+\Delta\beta\right)^{3/2}, \tag{21}$$

requires a different treatment. Instead of the treatment above, we assume now that a stationary shock forms over the front face of the forcing at $x=x'_m$ (Fig. 4). The structure to the left of this shock is similar to that described above:

$$\phi(u) = -\Delta u + \frac{\alpha u^2}{2} + \frac{\beta u^3}{3} = -C - f, \quad x < x'_m,$$

where

$$-C = f_m + g(\Delta), \quad g(\Delta) = \phi(u_m). \tag{22}$$

Then as $x=x'_m$, it is clear from Fig. 3 that $u=u'_m$ [see Eq. (16)], and this is sufficient to also determine x'_m. Then since the shock speed is now zero, one has $\phi(u'_m)=\phi(u''_m)$, which determines u''_m. Downstream of the shock ($x>x'_m$) one seeks a steady solution where $u \to u'_+$ as $x \to \infty$, and $u \to u''_m$ as $x \to x'_m+$. It is readily shown that this is also given by Eq. (22), so that, in fact, $u'_+ = u_-$, i.e., the downstream steady-state level is identical to that upstream. However, in the downstream case, this is not a shock, and instead is resolved by a rarefaction wave.

IV. NUMERICAL COMPUTATIONS

We now discuss some numerical studies of the forced eKdV equation for various flow regimes. A numerical code is developed using the Adams–Bashforth–Moulton predictor and corrector method to integrate Eq. (1) forward in time, and central finite difference formulas are employed in the spatial discretization process. The code is validated by comparing the numerical result with the exact solitary wave solutions of the eKdV equation.

The localized forcing is switched on impulsively when the time integration starts. We keep α constant ($\alpha=2$), and fix the forcing to be given by Eq. (2) for all simulations. Then Δ and β are varied to generate different flow regimes. In a subsequent discussion, the ''mass'' of the system is defined to be the area between the interfacial displacement and the undisturbed mean position. For two-dimensional flow, this volume, or area per unit depth, will represent the mass except for a constant factor equal to the density of the fluid. In order to study the mass fluctuation in front of and behind the forcing, we split the mass of the whole system into two parts, namely, $-\infty < x < 0$ (M_{front}) and $0 \leqslant x < +\infty$ $\times (M_{\text{behind}})$. As the total mass of the system is conserved, $M_{\text{front}} + M_{\text{behind}} = M_{\text{total}} = 0$ since the null initial condition is used here.

A. Part 1, forced eKdV, $\beta > 0$

1. Case (A): $\Delta < 0$

The transcritical range for Δ is defined by Eq. (20), which depends on f_m, α, and β. One particular value of β, namely, $\beta=1.4$, will be chosen for the purpose of discussion. The transcritical range is then given by $-0.71 < \Delta < 2.35$.

We first consider a large negative value of Δ ($\Delta=-3$) that is outside the transcritical regime. Figure 5(a) shows a typical solution of Eq. (1) with $\xi=0.3$, and $f_m=1$. The critical value of β found from Eq. (18) is given by $\beta_c=0.28$, and so there is no steady hydraulic solution available, since here $\beta > \beta_c$. Nevertheless, this case is quite similar to that of the usual forced KdV equation.[8] A localized stationary depression is observed just downstream of the forcing region followed by a stationary lee wavetrain. A solitary wavetrain is generated in the upstream direction with one very dominant

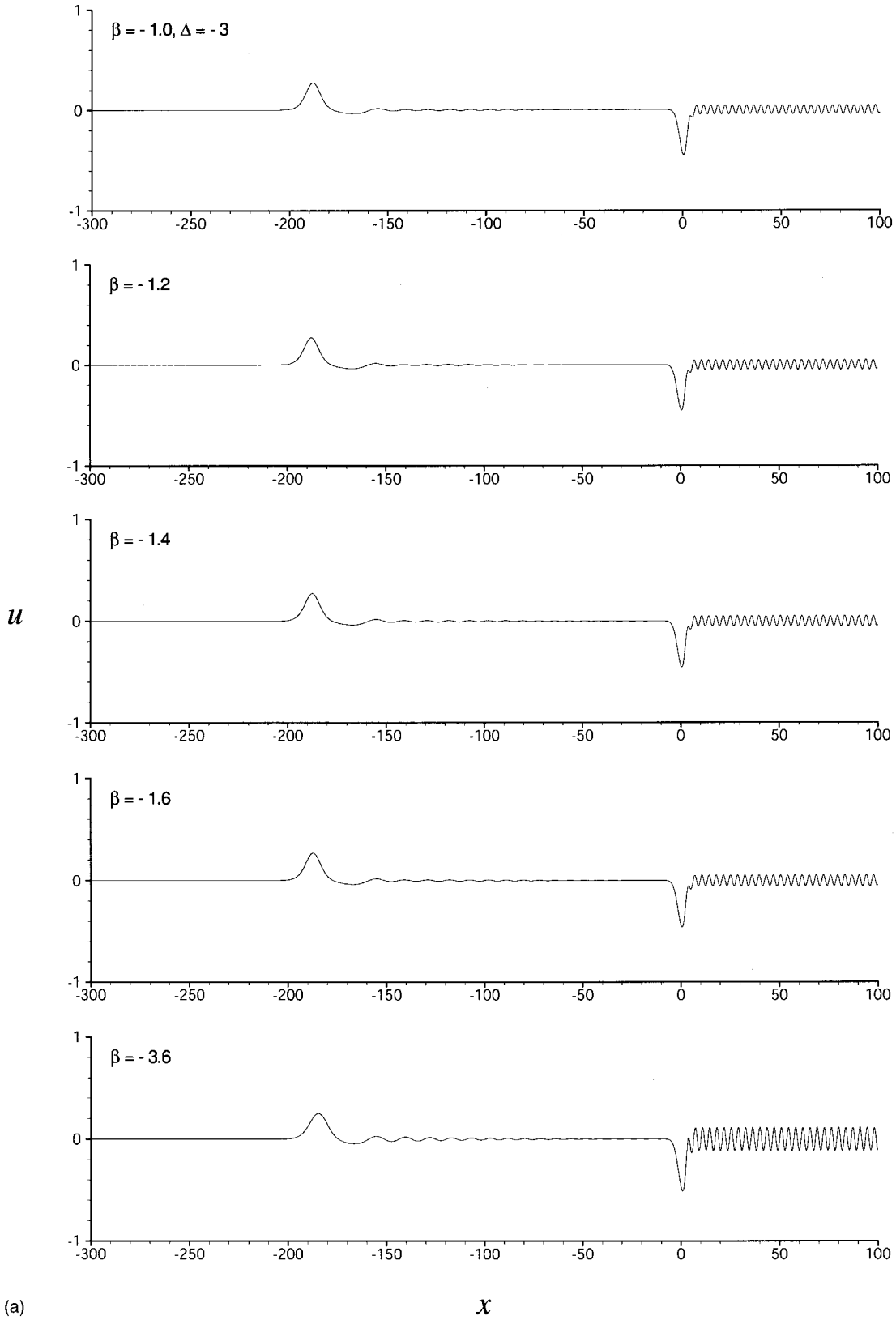

FIG. 9. (a) The interfacial displacement at $t=60$ with $\Delta=-3.0$, $f_m=1.0$, and $\xi=0.3$ for $\beta<0$. (b) The numerical solution with $\Delta=-3.0$, $\beta=-1.4$, $f_m=1.0$, and $\xi=0.3$.

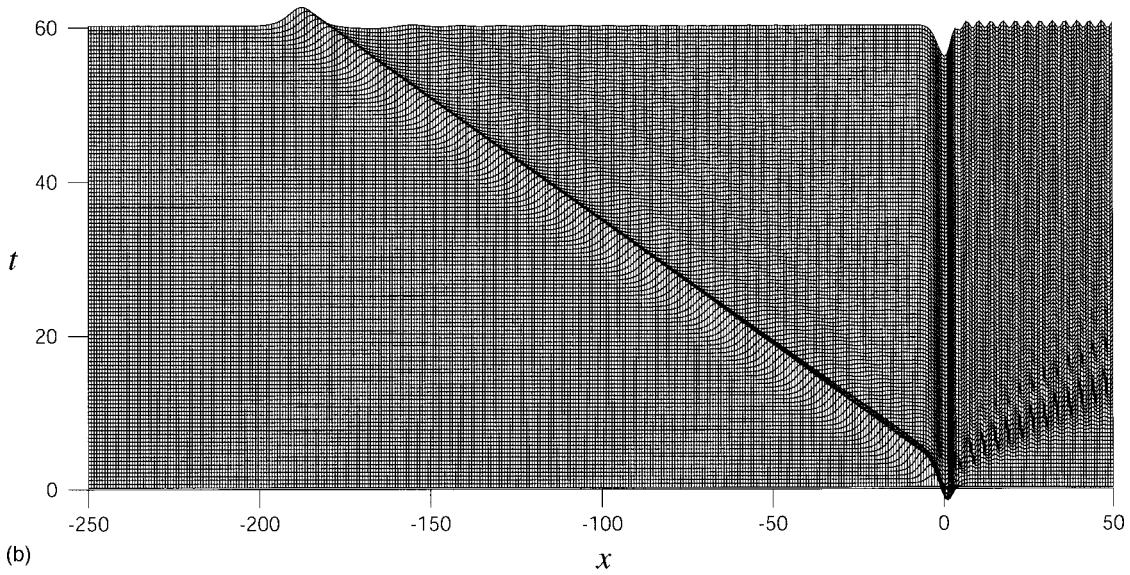

FIG. 9. (*Continued.*)

.

leading wave. The upstream solitary wave, formed at a very early stage, attains a mass of six units very soon after the integration starts. The total mass of the system is conserved and stays equal to zero steadily as time proceeds. Outside the transcritical regime, the introduction of the cubic nonlinearity does not generate any dramatic influence on the solution, as compared with the usual forced KdV model.

Next, we consider a case closer to the transcritical regime, $\Delta=-1$, but still with $\xi=0.3$ and $\beta=1.4$ [Fig. 6(a)]. There is now an undular bore upstream, although the oscillatory wave train downstream is the dominant feature. The critical value of β given by Eq. (18) here is $\beta_c=0.59$, and also $\beta>\beta_c$. It is therefore not surprising that there is no stationary depression just downstream of the forcing region. Instead, there is a downstream wavetrain, which is highly oscillatory. The characteristics obtained from Eqs. (4) are shown in Fig. 6(b). There are two shocks formed, one upstream that leads to the observed undular bore in Fig. 6(a), while the other is over the forcing and leads to the unsteadiness of the downstream wave train. Figure 6(c) shows the interfacial displacement at $t=60$, revealing the regime transitions as β is increased. At $\beta=0.3$, well below β_c, the solution is similar to that for the usual forced KdV equation, with an upstream undular bore, a depression just behind the obstacle, followed by a modulated wave train. This behavior persists until $\beta>\beta_c$, and for $\beta=0.6$ we see some variability in the downstream wave train, possibly indicative of a rarefaction type of modulation. On further increasing the value of β beyond β_c, the irregular oscillatory wave train becomes the dominant feature downstream while the number of upstream waves in the undular bore decreases.

2. Case (B): $\Delta=0$

We now consider the resonant case of $\Delta=0$, $\xi=0.3$ and $f_m=1$, where the critical value $\beta_c=1.15$. For $\beta>\beta_c$, our numerical computations show good agreement with the hydraulic approximation in that there is an upstream undular bore composed of solitary waves of nearly uniform amplitude, a stationary downstream depression terminated by a modulated wave train. The scenario is analogous to that described by GS for the forced KdV equation. Figure 1 shows the interfacial displacement at $t=60$ for different values of β. When β is only slightly greater than the critical value ($\beta=1.2$), the downstream depressed region ceases to exist, and instead a localized minimum develops. There are still regularly generated solitary waves upstream, and a modulated downstream wave train remains. On further increasing the value of β, two systems of upstream solitary waves are observed. They are regular ones, which are generated at an early stage and irregular ones, which are apparently generated in accordance with the fluctuations in the depression just in the lee of the forcing region. These irregular solitary waves, and the accompanying irregularly downstream waves are the most striking results of the present work, and differ drastically from the forced KdV model.

When the cutoff criterion [Eq. (18)] is exceeded (i.e., $\beta>\beta_c$), one can construct another steady hydraulic solution. This new solution has a stationary shock on the downstream side of the forcing, and is followed by a transition to a rarefaction. In the full equation (1) we interpret the presence of the stationary shock with the fluctuations seen just in the lee of the forcing, leading to the irregular generation of the higher-amplitude solitary waves (HASW) observed in the numerical computations, while the rarefaction becomes a rather weak downstream wave train. In this regime, we find that the hydraulic approximation is again useful in predicting the criterion for the presence of a steady lee depression, which is directly related to the structure of the upstream solitary waves. For $\beta=1.4$, five regular and two irregular HASWs are generated at $t=60$. The time development in the numerical computation for $\beta=1.4$ is shown in Fig. 7(a). The first HASW, generated at $t\approx30.5$, travels faster than the regularly generated solitary waves and interacts with them. We are proposing that the generation of this kind of HASW

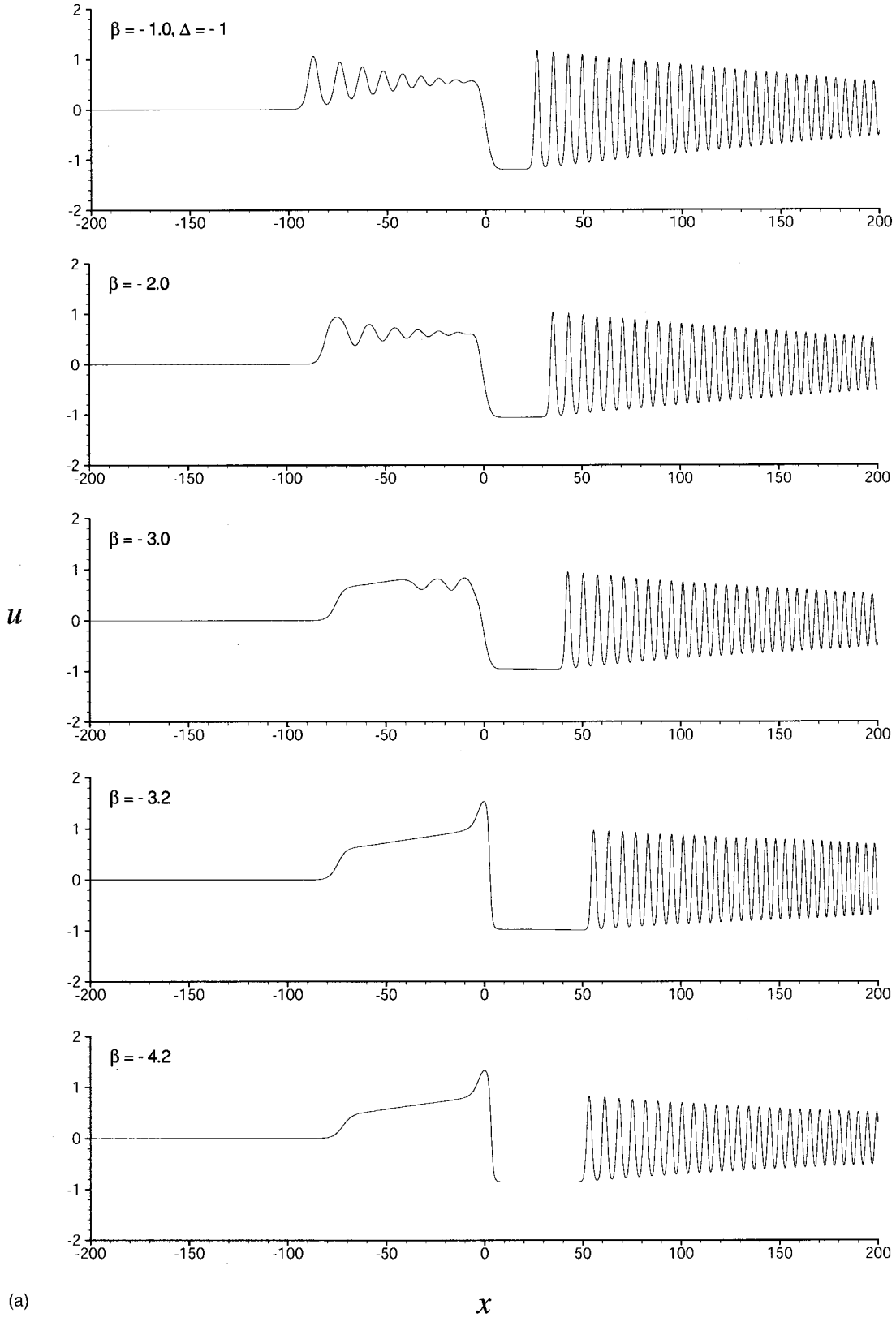

FIG. 10. (a) The interfacial displacement at $t=60$ with $\Delta=-1.0$, $f_m=1.0$, and $\xi=0.3$ for $\beta<0$. (b) The numerical solution with $\Delta=-1.0$, $\beta=-3.2$, $f_m=1.0$, and $\xi=0.3$.

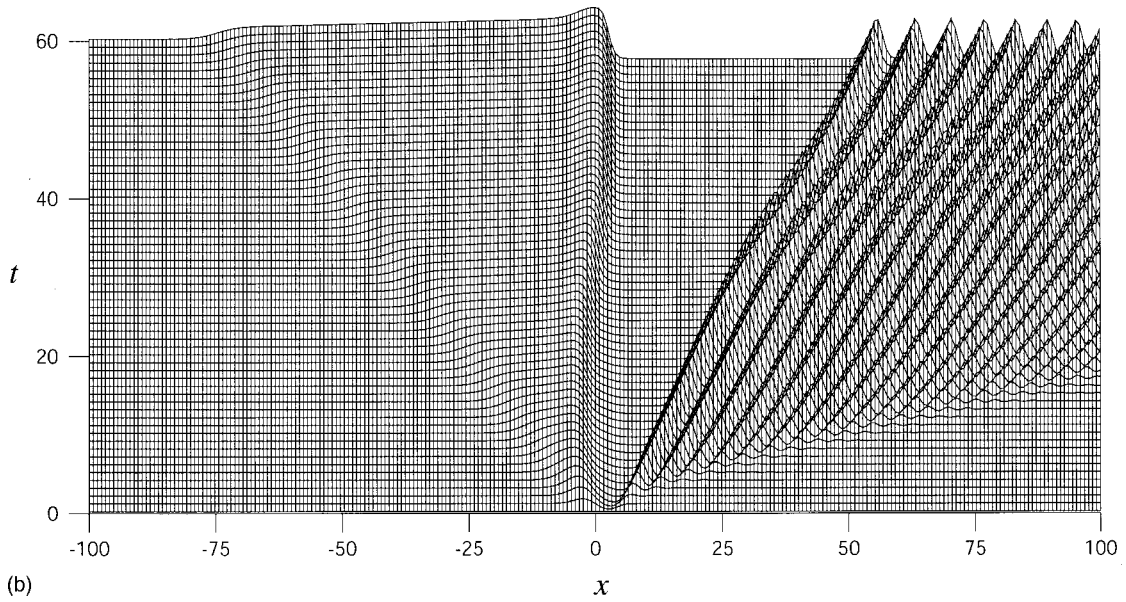

FIG. 10. (*Continued.*)

is due to the presence of a stationary shock on the downstream side of the forcing in the hydraulic approximation. Simultaneously, an oscillatory wave train is sent downstream. Once the localized depressed region possesses enough negative mass, it is apparently pushed upstream and undergoes a transformation. Simultaneously, one can recognize several fluctuations of mass in the upstream region [Fig. 7(b)], i.e., M_{front}, is no longer a straight line. If these localized and large negative disturbances near the forcing region have insufficient mass, they will decay into radiation and be sent back downstream. Figure 7(c) illustrates the characteristics for the case of $\beta=1.4$, which shows evidence to support these interpretations. Some characteristics curves, from the downstream side of the forcing region, bend toward the upstream direction, and have more than one turning point. When we increase the value of β to 1.6 (Fig. 1), the number of regularly generated solitary waves drops to three. For $\beta=3.6$, only one regular solitary wave is formed at an early stage. Consequently, we infer that increasing the cubic nonlinearity hinders the generation of the regular solitary waves, and at the same time triggers the formation of the HASWs.

3. Case (C): $\Delta>0$

Figure 8(a) shows the interfacial displacement at $t=60$ for different values of β with $\Delta=1$, $\xi=0.3$, and $f_m=1$. This is still in the transcritical regime, while $\beta_c=3.67$. For the fixed time period chosen the number of solitary waves generated is proportional to the value of β before it reaches the cutoff criterion of 3.67. When β exceeds the critical value, the depression cannot be maintained, and according to our hydraulic approximation, a stationary shock is formed behind the forcing region. Some HASWs are also observed for the case of $\beta=4.2$. Figure 8(b) shows the time history of the case $\beta=4.2$. Shocks will be needed if the characteristic curves intersect. Stationary shocks develop just behind the forcing region, and they form upstream advancing HASWs.

Finally, consider the case $\Delta=2$, $\xi=0.3$, and $f_m=1$, which is also in the transcritical regime, while $\beta_c=0.38$. This case shown in Fig. 8(c), illustrates the nonlinear character of the solitary wave formation. The generation period decreases and the number of the solitary waves increases if we choose a larger value of β [Fig. 8(c)], but are all still the irregular regime. However, the amplitudes of the solitary waves generated decrease from about 3.2 at $\beta=1.2$ to about 2.4 at $\beta=3.6$.

For an example outside the transcritical range, let $\Delta=3$, $\beta=1.4$, $\xi=0.3$, and $f_m=1$. A locally stationary elevation forms over the forcing region, and a downstream modulated wave train is obtained [Fig. 8(d)].

B. Part 2, eKdV, $\beta<0$

1. Case (A): $\Delta<0$

We first consider $\Delta=-3$, $\xi=0.3$, and $f_m=1$. Figure 9(a) shows a series of interfacial displacements at $t=60$. The cutoff criterion for this case is $\beta_c\approx-48.99$, so that we must have $|\beta|<|\beta_c|$ to have a steady hydraulic solution. Only one upstream solitary wave is generated and a depression develops in the forcing region. These results are quite similar to those of the forced KdV equation, and indeed Fig. 9(b) shows the time history of the case $\beta=-1.4$, which is very similar to the result of the case $\beta=+1.4$ (Fig. 5).

For $\Delta=-1$, there is a transition from the undular bore solution to the monotonic bore solution as $|\beta|$ is increased. Figure 10(a) shows quite dramatically a series of pictures representing this transition. The undular bore solution is obtained for $\beta=-1.0$ and the monotonic bore solution is found for $\beta=-3.2$; here $\beta_c\approx-3.67$ and so $|\beta|<|\beta_c|$ implies that the steady hydraulic solutions hold. But, as $|\beta|$ increases, the resolution of the upstream shock into an undular bore becomes instead resolution into a monotonic bore. Even when $|\beta|>|\beta_c|$, e.g., $\beta=-4.2$, the monotonic bore solution can

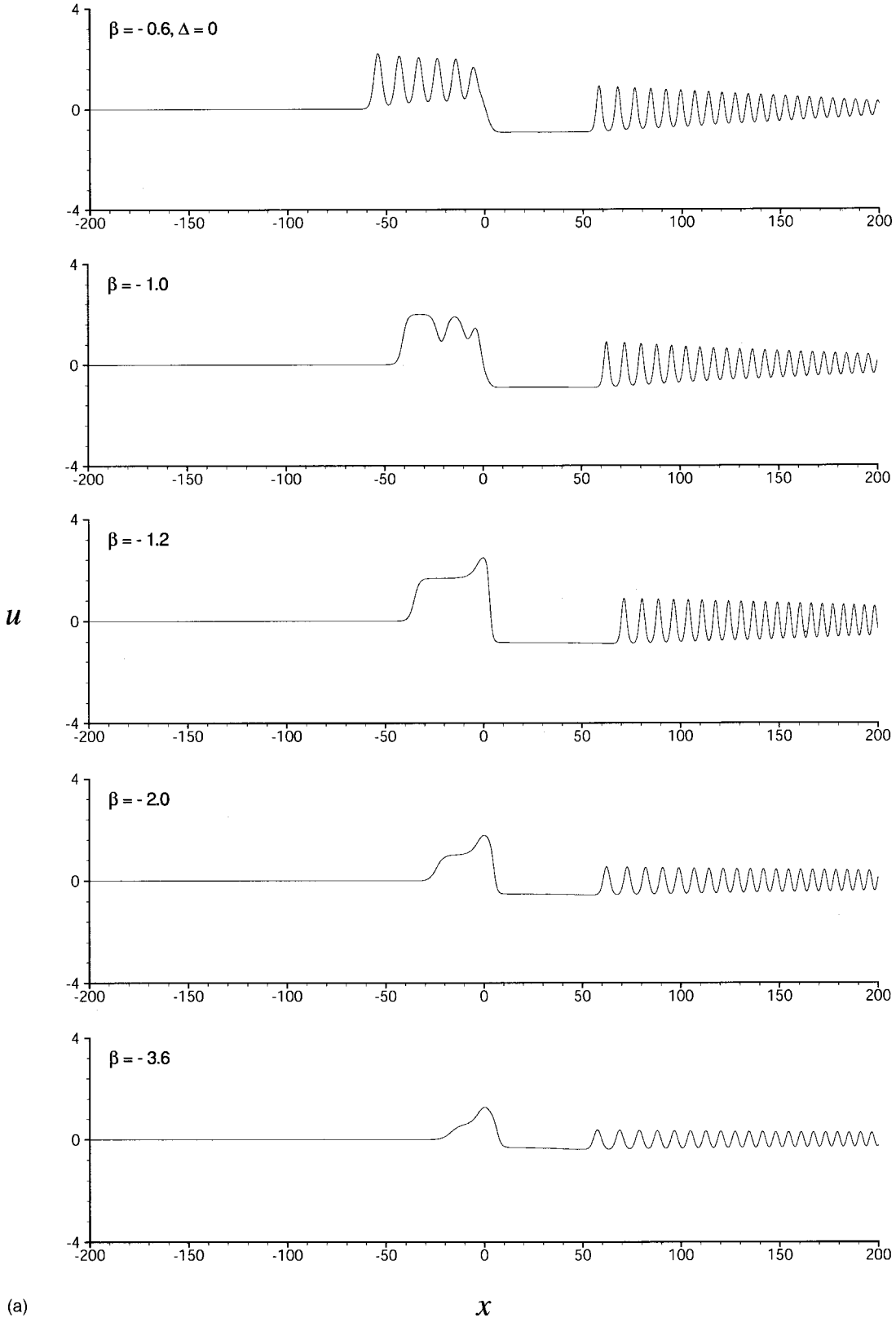

FIG. 11. (a) The interfacial displacement at $t=60$ with $\Delta=0$, $f_m=1.0$, and $\xi=0.3$ for $\beta<0$. (b) The numerical solution with $\Delta=0$, $\beta=-1.4$, $f_m=1.0$, and $\xi=0.3$.

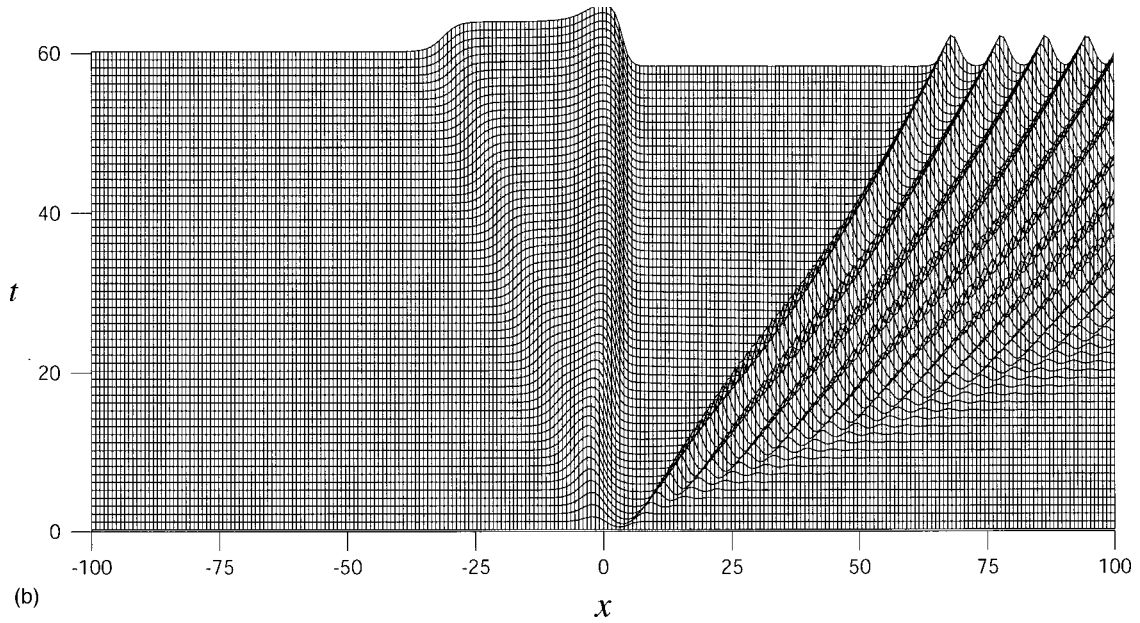

FIG. 11. (*Continued.*)

still be observed. The undular and monotonic bore solutions are globally unsteady, but do ultimately give new locally steady conditions immediately upstream of the forcing region.[5] Earlier work in the literature[1,5,6] shows that the qualitative form of the solution depends on the Froude number (Δ in our case) and the strength of the forcing. We find here that it also depends on the strength of the cubic nonlinearity. The time history for a particular value of β, $\beta \approx -3.2$, is shown in Fig. 10(b).

2. Case (B): $\Delta = 0$

This case is shown in Figs. 11(a) and 11(b), where now $\beta_c = -1.15$. However, even for $|\beta| > |\beta_c|$ (say $\beta = -2.0$ or $\beta = -3.6$), a monotonic bore solution is still found. A transition similar to that for the case $\Delta = -1$ is also obtained in this regime, in that as $|\beta|$ decreases, the upstream monotonic bore becomes an undular bore, e.g., an undular bore is observed at $\beta = -0.6$. But note that the structure of the upstream monotonic bore changes near the forcing, once the cutoff criterion is reached [Fig. 11(a)]. The hydraulic approximation is highly effective and precise in predicting the transition point in this case. Figure 11(b) shows the time history of the monotonic bore solution with $\beta = -1.4$.

3. Case (C): $\Delta > 0$

In Fig. 12 we consider $\Delta = 1$, which is within the transcritical regime, while $\beta_c = -0.59$. For $\beta = -0.3$ (below the cutoff criterion), three well-developed upstream solitary waves are emitted. A stable depression just behind the forcing is found. Further increasing $|\beta|$ results in a stable solution of elevation at the forcing. The amplitude of the elevation continues to decrease as one increases the numerical values β (Fig. 12). The time history for the case $\Delta = 1$ and $\beta = -1.4$ shows one single, localized elevation stationary at the location of the forcing.

For $\Delta = 3$, a steady supercritical solution is obtained for all the simulations within and outside of the steady depression regime (Figs. 13), as the value of Δ considered in this case is outside the transcritical range. A localized elevation is generated and located at the forcing with constant amplitude (≈ 0.35) for the different values of β considered. The amplitude of the elevation is quite insensitive to changes in β, in marked contrast with the previous case.

V. CONCLUSIONS

Transcritical flows of a stratified fluid over topography are considered using a forced extended Korteweg–de Vries model (eKdV). In the present paper we extend the earlier studies by allowing the cubic nonlinear and dispersive terms to have the same sign for their coefficients. A hydraulic approximation (HA) is developed by ignoring the dispersion term. This simplified model of the dynamics is shown to agree remarkably well with independent, direct numerical computations (DNC) of the full forced eKdV over most parameter regimes. A very interesting result is that two kinds of solitary waves are emitted in certain parameter regimes. Besides the regularly generated ones similar to those in the forced KdV model, there are irregularly generated solitary waves of variable amplitudes. The velocities of the two types of waves are different, and interactions among them are observed.

A further contribution of the present work is to unite these two approaches (HA and DNC) to enhance the understanding of the underlying fluid physics. More precisely, the hydraulic approximation computes a cutoff criterion for the absence of a downstream depression, a lower bound for Δ for any such hydraulic solution, and a determination of the transcritical regime. Indeed, we claim that once this cutoff criterion is exceeded, one can construct another steady hydraulic solution. This new steady solution has a stationary shock on

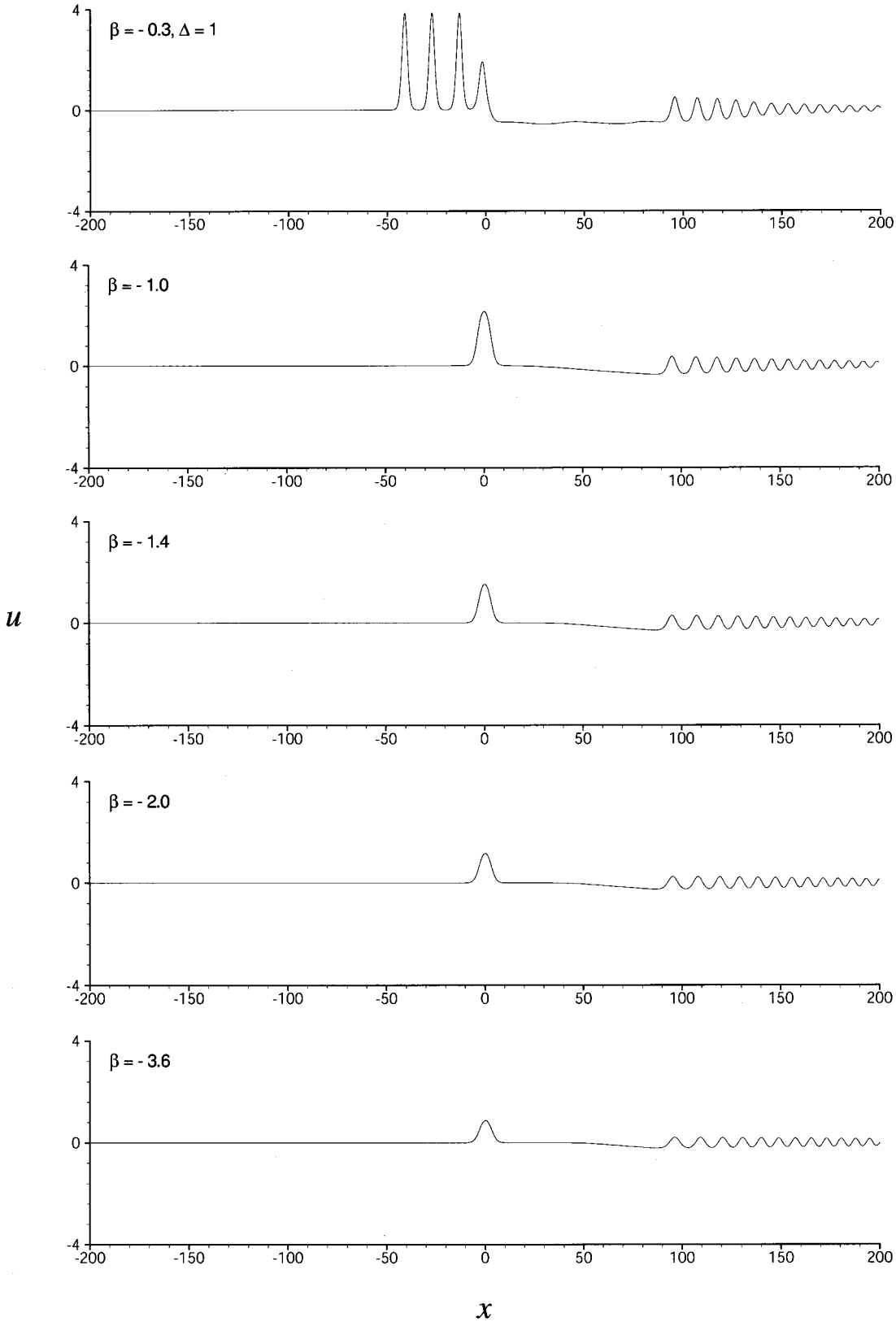

FIG. 12. The interfacial displacement at $t=60$ with $\Delta=1.0$, $f_m=1.0$, and $\xi=0.3$ for $\beta<0$.

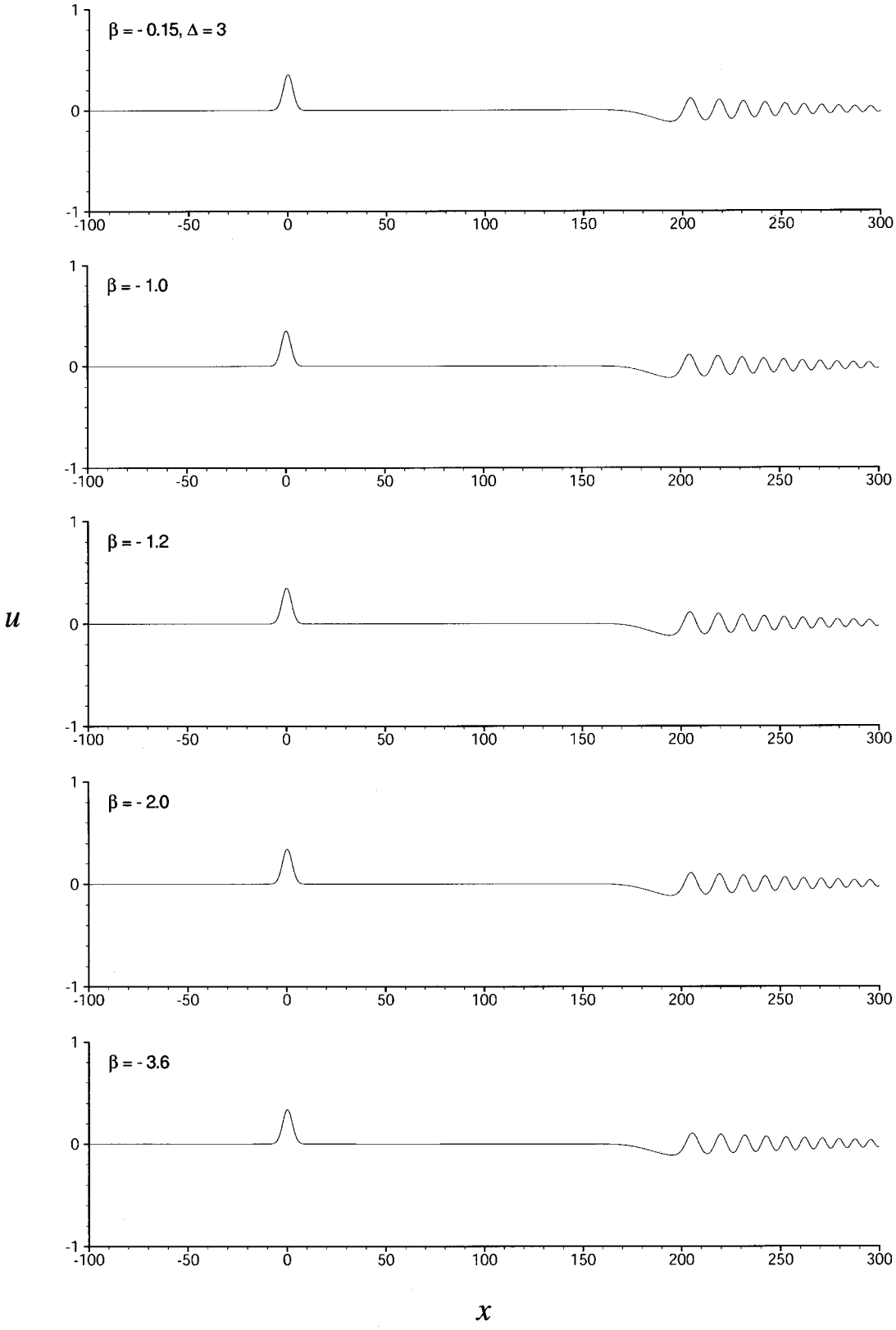

FIG. 13. The interfacial displacement at $t=60$ with $\Delta=3.0$, $f_m=1.0$, and $\xi=0.3$ for $\beta<0$.

the downstream side of the forcing, and is followed by a transition to a rarefaction. The stationary shock is associated with the irregular, large waves observed in the numerical results, while the rarefaction becomes a rather weak downstream wave train. Otherwise the upstream propagating shock that terminates the upstream steady hydraulic solution becomes the observed upstream train of solitary waves, and likewise downstream when the hydraulic solution extends downstream.

We consider briefly the more usual case where the cubic and dispersive terms have opposite signs, and the hydraulic approximation are demonstrated to work there as well. Only positive forcing has been considered here. The effects of negative forcing will be reported in a future work.

ACKNOWLEDGMENT

Partial financial support has been provided by the Research Grants Council Contracts No. HKU 7067/98E and No. HKU 7066/00E.

[1]R. H. J. Grimshaw, ''Internal solitary waves,'' *Advances in Coastal and Ocean Engineering*, edited by P. L.-F. Liu (World Scientific, Singapore, 1997), Vol. 3, pp. 1–30.
[2]P. E. Holloway, E. Pelinovsky, T. Talipova, and B. Barnes, ''A nonlinear model of the internal tide transformation on the Australian North-West shelf,'' J. Phys. Oceanogr. **27**, 871 (1997).
[3]H. Michalet and E. Barthelemy, ''Experimental study of interfacial solitary waves,'' J. Fluid Mech. **366**, 159 (1998).
[4]R. Grimshaw, E. Pelinovsky, and T. Talipova, ''Solitary wave transformation in a medium with sign-variable quadratic nonlinearity and cubic nonlinearity,'' Physica D **132**, 40 (1999).
[5]W. K. Melville and K. R. Helfrich, ''Transcritical two-layer flow over topography,'' J. Fluid Mech. **178**, 31 (1987).
[6]T. R. Marchant and N. F. Smyth, ''Extended Korteweg–de Vries equation and the resonant flow of a fluid over topography,'' J. Fluid Mech. **221**, 263 (1990).
[7]H. Hanazaki, ''A numerical study of nonlinear waves in a transcritical flow of stratified fluid past an obstacle,'' Phys. Fluids A **4**, 2230 (1992).
[8]R. H. J. Grimshaw and N. F. Smyth, ''Resonant flow of a stratified fluid over topography,'' J. Fluid Mech. **169**, 429 (1986).
[9]T. R. Marchant, ''Coupled Korteweg–de Vries equations describing, to high order, resonant flow of a fluid over topography,'' Phys. Fluids **11**, 1797 (1999).
[10]R. H. J. Grimshaw, E. Pelinovsky, and T. Talipova, ''The modified Korteweg–de Vries equation in the theory of large amplitude internal waves,'' Nonlinear Processes in Geophys. **4**, 237 (1997).
[11]J. W. Choi, S. M. Sun, and M. C. Shen, ''Internal capillary-gravity waves of a two-layer fluid with free surface over an obstruction—Forced extended KdV equation,'' Phys. Fluids **8**, 397 (1996).
[12]J. W. Rottman, D. Broutman, and R. H. J. Grimshaw, ''Numerical simulations of uniformly-stratified fluid flow over topography,'' J. Fluid Mech. **306**, 1 (1996).